Modeling a Temporally Evolving Atmosphere with Zernike Polynomials

Isaac B. Putnam
Air Force Institute of Technology, 2950 Hobson Way, WPAFB, OH 45433
Stephen C. Cain
Air Force Institute of Technology, 2950 Hobson Way, WPAFB, OH 45433

ABSTRACT

This paper develops a new, more accurate temporal model of phase screen generation. The long standing Fourier transform (FT) based method assumes the frozen flow hypothesis holds, where large phase screens are generated and then shifted. The result is a statistically correct screen. Realistically however, the phase changes with time, especially when the wind velocity is small or non-existent. The temporal evolution method proposed in this paper is based on expanding a random walk algorithm to the Zernike polynomial method that will include not only the perceived shifting of the Kolmogorov FT method, but also a "boiling effect" that changes the phase as it shifts. This new method of phase screen generation will be validated through a simulated experiment which measures the correlations of tilt as a function of time and compares that to a predicted tilt correlation function derived using both the frozen flow hypothesis and the new model. This validation experiment will show that the frozen flow model alone fails to accurately predict the temporal correlation of optical tilt.

1. INTRODUCTION

For conventional imaging systems, Geosynchronous Earth Orbit (GEO) space objects cannot be resolved due to their 40 Mm distance. The need to obtain high resolution images of GEO objects is quite real and to accomplish this task, the Air Force Research Laboratories (AFRL) is currently investigating the suitability of inverse synthetic aperture laser radar (ISAL) at the Air Force Maui Optical and Supercomputing Site (AMOS). A critical component to determining its suitability is to accurately model the atmospheric impacts on LADAR pulses. The expected result is that atmospheric impacts are a strong function of the illumination wavelength, by the conventional knowledge that shorter wavelengths are more affected than longer ones. Conventional thinking is that while the atmosphere churns, wind is the predominant effect that simplifies all modeling and simulation into the frozen flow hypothesis. The concern is that frozen flow hypothesis based phase screen generation techniques fail to accurately predict the temporal correlation of optical phase in low wind velocity situations, thus the intent of this work is to develop a turbulent flow model. This "boiling effect" is the churning and fluctuation in realistic turbulence. We derive the temporal evolution aspect from [4] who applies a random walk to the first two Zernike polynomials, accurately simulating atmospheric tilt. Wave front phase aberrations introduced by the atmosphere are dominated by tilt, causing the most degradation of performance in direct-detection LADAR systems. This project expands upon [4]'s tilt algorithm; and is capable of including as many N number of Zernike polynomials as desired for low wind velocity environments.

2. BACKGROUND

We simulate atmospheric turbulence phase screens with MatLab through two common modeling approaches: modified von-Kármán, and Zernike polynomial-based phase screen generation. We initiate this investigation by introducing and defining the Fourier transform (FT) to which we compare our new Zernike-based method of temporal phase screen generation.

2.1 Fourier-based Phase Screen Generation

The FT methods are most common since very large phase screens can be generated quickly. Most FT methods are similar in that they are based on their respectively named power spectral density (PSD). One main downside is to this approach is that lower-order aberrations such as tilt are often under-represented [2]. These lower-order aberrations make up a majority of the atmospheric energy spectrum and as such, must be included to produce realistic models. One of the more widely used FT based methods is based on the von-Kármán spectrum,

$$\Phi(\kappa) = 0.023(r_0)^{-5/3} e^{-\left(\frac{\kappa}{\kappa_m}\right)^2} (\kappa^2 + {\kappa_0}^2)^{-11/6}. \tag{1}$$

The modified von-Kármán allows an estimation of the inner (l_0) and outer (L_0) scales of turbulent eddies, leading to $\kappa_m = 5.92/l_0$, and $\kappa_0 = 2\pi/L_0$, in which κ is spatial frequency and is scaled by a factor of Fried's constant, r_0. For this investigation we approximate ideal limits, L_0 approaches infinity and l_0 approaches zero. To better reflect the AMOS observatory, we select D to be 1.6 m and r_0 to be 14 cm. With these parameters we simplify Eq. (1) to Eq. (2).

$$\Phi(\kappa) = 0.023(r_0)^{-5/3} (\kappa^2)^{-11/6} \tag{2}$$

As FT-based methods are not the focus of this paper we limit our discussion to this point. For comparative analysis in subsequent sections we utilize Listing 9.2 from [2] to generate the von-Kármán phase screens.

2.2 Zernike-based Phase Screen Generation

Drawing a stark contrast to Fourier methods, the Zernike polynomial approach does not begin with a random phase array, instead the coefficients are combined into two-dimensional random functions. In his 1976 paper, Noll [6] defined a new modified set of Zernike polynomials $Z_j(p, \theta)$. He defined these polynomials to be

$$\left.\begin{aligned} Z_{even\ j} &= \sqrt{n+1} R_n^m \sqrt{2} \cos(m\theta) \\ Z_{odd\ j} &= \sqrt{n+1} R_n^m \sqrt{2} \sin(m\theta) \end{aligned}\right\}, \quad m \neq 0$$
$$Z_j = \sqrt{n+1} R_n^0(r), \quad m = 0 \tag{3}$$

where the functions $R_n^m(r)$ are referred to as radial functions defined to be

$$R_n^m(r) = \sum_{s=0}^{(n-m)/2} \frac{(-1)^s (n-s)!}{s!\,[(n+m)/2 - s]!\,[(n-m)/2 - s]!} r^{n-2s}. \tag{4}$$

Based on a polar coordinate system, R is the radius, p is the position along the radius, and θ is the angle with respect to the x-axis. Noll's numbering sequence of the index j corresponds to each polynomial Z_j and proceeds by row, then given value of radial degree n, and increases with azimuthal frequency m. We generate random phase screens, Θ_{atm}, from the relationship:

$$\Theta_{atm}(Rp, \theta) = \sum_j a_j Z_j(p, \theta). \tag{5}$$

To generate the phase screen with accurate correlation we calculate the amplitude a_j vector by multiplying $\underline{\underline{\Phi}}$ with a zero-mean, unit-variance random vector.

$$a_j = \underline{\underline{\Phi}} \vec{n} \tag{6}$$

$\underline{\underline{\Phi}}$ is the Cholesky decomposition of the covariance matrix

$$\underline{\underline{\Phi}} = \sqrt{C_{j,i}} \qquad \text{and} \qquad \underline{\underline{\Phi}}^{\mathrm{T}} \underline{\underline{\Phi}} = C_{j,i} \tag{7}$$

where the covariance matrix $C_{j,j'}$ is generated from the covariance of two Zernike polynomials Z_j and $Z_{j'}$ with amplitudes a_j and $a_{j'}$:

$$C_{j,j'} = E\left[a_j, a_{j'}\right] = \frac{K_{zz'} \delta_z \Gamma\left[\left(n + n' - 5/3\right)/2\right] (D/r_o)^{5/3}}{\Gamma[(n - n' - 17/3)/2] \Gamma[(n - n' - 17/3)/2] \Gamma[(n + n' - 23/3)/2]}, \tag{8}$$

in which

$$K_{zz'} = \frac{\Gamma(14/3)[(24/5)\Gamma(6/5)]^{5/6}[\Gamma(11/6)]^2}{2\pi^2} \times (-1)^{(n+n'-2m)/2}\sqrt{(n+1)(n'+1)}\,, \tag{9}$$

and

$$\delta_z = \left(m = m'\right) \bigwedge \left[\overline{parity(j,j')} \;\vee\; (m=0)\right]. \tag{10}$$

3. TEMPORAL CORRELATION

Without determining some factor of correlation between individual pixels, the FT methods cannot be evolved, only shifted with statistical accuracy. The benefit of the Zernike method however, is that once a single random screen is generated, the correlation between each pixel is inherent within the Zernike polynomials. Cain's [4] work with atmospheric tilt has already generated a statistically accurate algorithm to temporally evolve the first two Zernike polynomials. We expand the algorithm of the first two polynomials to any *N* maximum number of Zernike polynomials, and utilize the methodology of the expanded algorithm to generate a temporal correlation of the aforementioned $\vec{n}$ vector. With this temporal correlation we can evolve the a_j vector with accurate correlation of contiguous phase screens. We utilize Bayes' theorem to update the vector $\vec{n}$ with mean Eq. (11) and variance Eq. (12):

$$E[\vec{n}(t_2)|\vec{n}(t_1)] = \frac{\vec{n}(t_1)R_{\vec{n}}(\Delta t)}{Var\left(\vec{n}(t_1)\right)} \tag{11}$$

$$E\left[\left(\vec{n}(t_2) - \vec{n}(t_1)\frac{R_{\vec{n}}(\Delta t)}{\sigma_{\vec{n}}^2}\middle|\alpha_1\right)\right] = \frac{\sigma_{\vec{n}}^4 - R_{\vec{n}}^2(\Delta t)}{\sigma_{\vec{n}}^2} \tag{12}$$

and solve for the correlation of the $\vec{n}$ vector in time, $R_{\vec{n}}(\Delta t)$. We utilize the relationship in Eq. (11) to define the correlation between two $\vec{n}$'s as

$$R_{\vec{n}}(\Delta t) = E\left[\left(\sum_{k=1}^{N} \underline{\underline{\Phi}}_{\mathrm{k}}^{-1} a_k(t1)\right)\left(\sum_{l=1}^{N} \underline{\underline{\Phi}}_{\mathrm{l}}^{-1} a_l(t_2)\right)\right]. \tag{13}$$

We then build upon the definition of these a_j's from [4] and expand Eq. (13) by substituting in

$$\begin{aligned} a_k(t_1) &= \frac{\int\int A(w,s)\varphi_k(w,s)\Theta_{atm}(w,s)dwds}{\int\int A(w,s){\Phi_k}^2(w,s)\partial w\partial s} \\ a_l(t_2) &= \frac{\int\int A(w,s)\varphi_l(w,s)\Theta_{atm}\left(w+(v_x)\Delta t, s+(v_y)\Delta t\right)\partial w_2\partial s_2}{\int\int A(w,s){\varphi_k}^2(w,s)\partial w\partial s} \end{aligned} \tag{14}$$

yielding

$$R_{\vec{n}}(\Delta t) = E\left[\begin{array}{c} \left(\sum_{k=1}^{N} \underline{\underline{\Phi}}_{\mathrm{k}}^{-1} \frac{\int\int A(w_1,s_1)\varphi_k(w,s)\Theta_{atm}(w_1,s_1)\partial w_1\partial s_1}{\int\int A(w,s){\varphi_k}^2(w,s)\partial w\partial s}\right) \times \\ \left(\sum_{l=1}^{N} \underline{\underline{\Phi}}_{\mathrm{l}}^{-1} \frac{\int\int A(w_2,s_2)\varphi_l(w_2,s_2)\Theta_{atm}\left(w_2+v_x\Delta t, s_2+v_y\Delta t\right)\partial w_2\partial s_2}{\int\int A(w,s){\varphi_l}^2(w,s)\partial w\partial s}\right) \end{array}\right]. \tag{15}$$

We have redefined our notation of the Zernike polynomials Z_j as φ_k and φ_l allowing for temporal correlation. Additionally we represent our aperture as *A*, and the atmospheric phase screen Θ_{atm}, each with the same coordinate

system (w,s). By rearranging, recognizing that the expectation operation is linear, and grouping similar terms we redefine Eq. (15)

$$R_{\vec{n}}(\Delta t) = \sum_{k=1}^{N}\sum_{l=1}^{N} \underline{\underline{\Phi}}_{\mathrm{k}}{}^{-1}\underline{\underline{\Phi}}_{\mathrm{l}}{}^{-1} \frac{\int\int\int\int A(w_1,s_1)A(w_2,s_2)\varphi_k(w_1,s_1)\varphi_l(w_2,s_2)}{\int\int A(w,s)\varphi_k{}^2(w,s)\partial w\partial s \int\int A(w,s)\varphi_l{}^2(w,s)\partial w\partial s} \times E[\Theta_{\mathrm{atm}}(w_1,s_1)\Theta_{atm}(w_2+v_x\Delta t, s_2+v_x\Delta t)]\partial w_1\partial s_1\partial w_2\partial s_2. \tag{16}$$

This is possible due to the fact that the first line in Eq. (15) is deterministic given the input parameters D, r_0, and the respective wind speeds. Recognizing that the expectation is a correlation we are able to redefine Eq. (16) as Eq. (17) by a change of variables, $\tau_x = w_2 - w_1$ & $\tau_y = s_2 - s_1$ and $\delta\tau_x = \delta w_2$, $\delta\tau_y = \delta s_2$

$$R_{\vec{n}}(\Delta t) = \sum_{k=1}^{N}\sum_{l=1}^{N} \underline{\underline{\Phi}}_{k}{}^{-1}\underline{\underline{\Phi}}_{l}{}^{-1} \frac{\int\int\int\int A(w_1,s_1)A\big(w_1+\tau_x,s_1+\tau_y\big)\varphi_k(w_1,s_1)\varphi_l\big(w_1+\tau_x,s_1+\tau_y\big)}{\int\int A(w,s)\varphi_k{}^2(w,s)\partial w\partial s \int\int A(w,s)\varphi_l{}^2(w,s)\partial w\partial s} \times R_\theta\big[(\tau_x+(v_x+v_b)\Delta t,\tau_y+(v_x+v_b)\Delta t)\big]\partial w_1\partial s_1\partial\tau_x\partial\tau_y. \tag{17}$$

We simplify the first line of the numerator as the independent multiplication of Zernike polynomials with the aperture

$$\begin{aligned} F &= A(w_1,s_1)\varphi_k(w_1,s_1) \\ G &= A\big(w_1+\tau_x,s_1+\tau_y\big)\varphi_l\big(w_1+\tau_x,s_1+\tau_y\big) \end{aligned} \tag{18}$$

which we then correlate using Fourier transform properties and define the inner double integral operation as $P_{k,l}$.

$$P_{k,l}(\tau_x,\tau_y) = \int_{\infty}^{\infty}\int_{\infty}^{\infty} A(w_1,s_1)\varphi_k(w_1,s_1)A\big(w_1+\tau_x,s_1+\tau_y\big)\varphi_l\big(w_1+\tau_x,s_1+\tau_y\big)\ \partial w_1\partial s_1 \tag{19}$$

This simplifies Eq. (17) to

$$R_{\vec{n}}(\Delta t) = \frac{D^2}{4\pi^2}\sum_{k=1}^{N}\sum_{l=1}^{N} \underline{\underline{\Phi}}_{k}{}^{-1}\underline{\underline{\Phi}}_{l}{}^{-1} \frac{\int\int P_{k.l}(\tau_x,\tau_y)R_\theta\big[(\tau_x+v_x\Delta t,\tau_y+v_x\Delta t)\big]\partial\tau_x\partial\tau_y}{\int\int A(w,s)\varphi_k{}^2(w,s)\partial w\partial s \int\int A(w,s)\varphi_l{}^2(w,s)\partial w\partial s}. \tag{20}$$

Unfortunately we do not have a method for computing the correlation of the atmospheric phase screens R_θ directly. Therefore we use the relationship of the phase structure to the phase correlation function [4]

$$D_{\vec{n}}(\Delta t) = 2R_{\vec{n}}(0) - 2R_{\vec{n}}(\Delta t). \tag{21}$$

We rearrange, add zero $(+R_\theta[0,0] - R_\theta[0,0])$ and substitute back into Eq. (20) giving

$$D_{\vec{n}} = \frac{D^2}{4\pi^2}\sum_{k=1}^{N}\sum_{l=1}^{N} \underline{\underline{\Phi}}_{\mathrm{k}}{}^{-1}\underline{\underline{\Phi}}_{\mathrm{l}}{}^{-1} \frac{\int\int P_{k.l}(\tau_x,\tau_y)2\begin{pmatrix} R_\theta[0,0]-R_\theta[0,0]+R_\theta\big[\tau_x,\tau_y\big]- \\ R_\theta\big[(\tau_x+v_x\Delta t,\tau_y+v_x\Delta t)\big]\end{pmatrix}\partial\tau_x\partial\tau_y}{\int\int A(w,s)\varphi_k{}^2(w,s)\partial w\partial s \int\int A(w,s)\varphi_l{}^2(w,s)\partial w\partial s} \tag{22}$$

By pairing the phase variances with the appropriate phase correlations, recalling Eq. (21), the structure function can be expressed in terms of a phase structure function difference.

$$D_{\vec{n}} = \frac{D^2}{4\pi^2}\sum_{k=1}^{N}\sum_{l=1}^{N} \underline{\underline{\Phi}}_{\mathrm{k}}{}^{-1}\underline{\underline{\Phi}}_{\mathrm{l}}{}^{-1} \frac{\int\int P_{k.l}(\tau_x,\tau_y)\big[D_\theta\big(\tau_x+v_x\Delta t,\tau_y+v_x\Delta t\big)-D_\theta\big(\tau_x,\tau_y\big)\big]\partial\tau_x\partial\tau_y}{\int\int A(w,s)\varphi_k{}^2(w,s)\partial w\partial s \int\int A(w,s)\varphi_l{}^2(w,s)\partial w\partial s} \tag{23}$$

[4] provides the methodology to analytically calculate the phase structure difference for the aforementioned inputs. We can now solve for $D_{\vec{n}}$, and by the relationship of Eq. (21) solve for $R_{\vec{n}}$. With $R_{\vec{n}}$ calculated for a given N

polynomials, D, r_0, and wind speeds v_x & v_y, we can accurately update the random $\vec{n}$ vector with Eq. (11) and Eq. (12). This allows us to temporally evolve the phase screen $\phi(Rp,\theta)$ with the correct correlation quickly, since the $R_{\vec{n}}$ vector only needs to be generated once for any given condition. While computationally it is inefficient to regenerate the $R_{\vec{n}}$ vector each time a simulation is performed, having a database of stored vectors allows for very efficient phase screen generation with the accurate correlation. In contrast to the frozen flow method in which a large phase array must be generated and then shifted, this Zernike-based turbulent flow method requires only the correlation matrix, $C_{j,j'}$, the correlation vector, $R_{\vec{n}}$, and the Zernike polynomials, Z_j to be stored. The update then becomes an extremely fast matrix operation, and does not require an enormous amount of memory and processing time to store and shift giant phase arrays.

4. ANALYSIS

To validate this turbulent flow approach to temporal evolution we focus on two metrics: temporal tilt correlation in time, and the long exposure optical transfer function (OTF). [4] provides the methodology to calculate the theoretical tilt correlation given input parameters D, r_0, and wind speeds v_x & v_y, and is based on the accepted thin lens approximation phase structure of the atmosphere. We present this as the theoretical basis for our x & y tilt in time analysis.

$$\alpha_{x,y}(t_n) = \frac{\int_{\infty}^{\infty}\int_{\infty}^{\infty} A(w,s)\theta_{atm}(w,s,t_n)\varphi_{x,y}(w,s)}{\int_{\infty}^{\infty}\int_{\infty}^{\infty} A(w,s)\,\varphi_{x,y}^2(w,s)} \tag{24}$$

The tilt $\alpha_{x,y}$ is calculated from the first two Zernike's $\varphi_{x,y}$ which correspond to x and y tilt respectively, the aperture A, and instant draws of our successive Zernike and FT-based phase screens θ_{atm}. Since tilt is zero mean [4], to calculate the correlation of these tilts in time we recognize that

$$R_{\alpha}(t_1,t_2) = E\left[\alpha_{x,y}(t_1),\alpha_{x,y}(t_2)\right] \tag{25}$$

and average thirty simulations to produce our mean μ measured tilt correlations in time. We performed this analysis on four different low wind-velocity conditions and averaged our results to calculate the mean μ and standard deviation σ^2. We present our simulated measurements for comparison to the theoretical (underlined) values in Table 1.

Table 1. Monte Carlo tilt correlation results

	X Correlation					*Y Correlation*				
	von-Kármán μ	σ^2	Zernike μ	σ^2	Theory μ	von-Kármán μ	σ^2	Zernike μ	σ^2	Theory μ
V_x =0.125	17.873	5.752	24.120	5.862	26.028	16.001	5.589	25.791	9.434	26.0289
V_y =0.125		5.971		5.971			5.971		5.971	
V_x =0.25	14.1568	3.486	24.653	6.464	25.5015	14.706	6.088	26.949	9.948	26.0308
V_y = 0.0		4.655		4.655			4.752		4.752	
V_x =0.25	13.51712	4.935	25.113	4.745	24.6239	10.868	3.289	23.123	2.243	23.299
V_y = 0.5		4.495		4.495			4.253		4.253	
V_x =0.75	8.61027	3.519	20.454	2.046	20.6438	9.369	4.071	22.620	3.32	22.2606
V_y = 0.5		3.734		3.734			4.129		4.129	

This analysis clearly shows that the turbulent flow Zernike-based approach significantly outperforms the frozen flow von- Kármán-based approach, in regards to temporal tilt correlation. The von-Kármán measurements provided for each wind based scenario depict that in all cases the measured mean is off from the theoretical mean by a factor

greater than one standard deviation. Additionally, all Zernike measurements fit well to the theoretical mean and are well within a standard deviation of the theoretical mean.

Next we examine the long exposure OTF. We generate the theoretical OTF as a product of the diffraction limited OTF and Eq. (26), [5]. The diffraction limited OTF is generated by the FT of the point spread function (PSF) created by the pupil function with zero phase.

$$\mathcal{H}_{\mathrm{L}}(v) = e^{-3.44\left(\frac{\lambda f v}{r_o}\right)^{5/3}} \tag{26}$$

To simulate the measured long exposure OTF we simulate more than five hundred iterations of the temporal evolution, both frozen flow and turbulent flow, capture the instantaneous OTF, and average the instantaneous OTFs. The average OTFs are then compared to the theoretical long-exposure OTF [5] and quantified via mean squared error (MSE) analysis. Our Monte-Carlo MSE results are provided in Table 2.

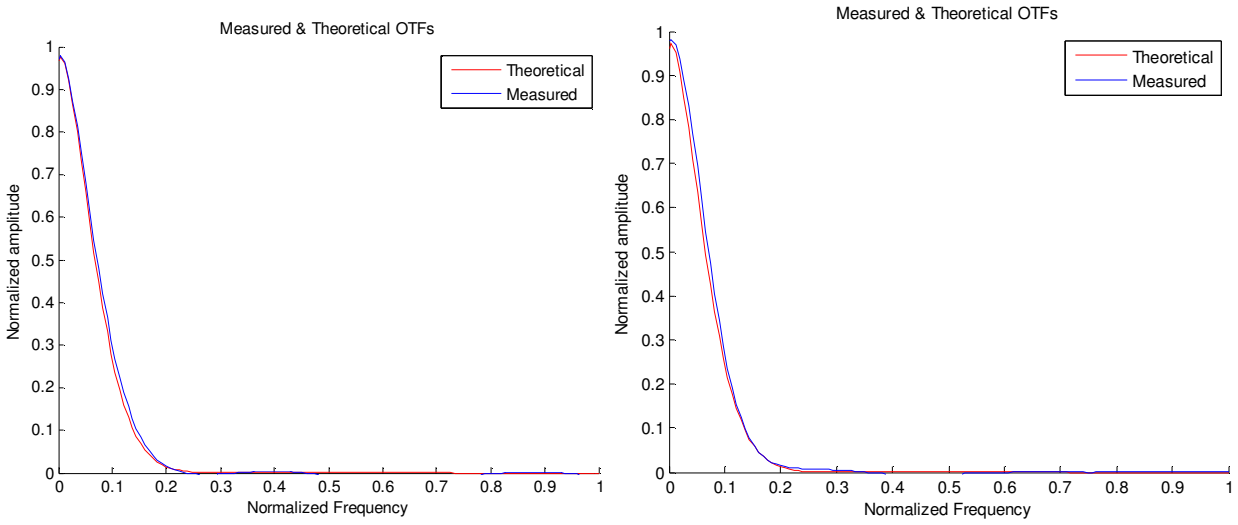

(a) **(b)**

Fig. 1: Long-exposure OTF compared to measured: (a) modified von-Kármán frozen flow OTF, (b) Zernike turbulent flow OTF

Table 2. Mean-Squared Error results

	MSE	
	von-Kármán	Zernike
V_x =0.125 V_y =0.125	1.17E-04	2.94E-04
V_x =0.25 V_y = 0.0	2.97E-04	1.46E-04
V_x =0.25 V_y = 0.5	1.18E-04	9.08E-05
V_x =0.75 V_y = 0.5	8.96E-05	7.51E-05

In addition to our findings on temporal tilt correlation in time, we see from the long exposure OTF that this new turbulent flow model is comparably accurate to the standard frozen flow model. Finally we note that computational time for each simulation, if treated independently, is comparably the same. However as previously alluded to, the Zernike-based approach described in this paper allows for $R_{\vec{n}}$ to be calculated once for any given conditions. With

the $R_{\vec{n}}$ vector already populated, the turbulent flow model produces temporal phase screens considerably faster than frozen flow model does.

5. CONCLUSION

Through the analysis provided above, we have generated a method of turbulent flow phase screen generation. We have shown that a random phase screen generated in a conventional manner can be temporally evolved for low wind velocity situations using this Zernike polynomial-based approach. This temporal evolution of phase as the screen slowly shifts has been validated through statistical analysis. We compared this approach to a widely used frozen flow approach and highlighted the turbulent flow's significant outperformance. Finally, having developed, tested, and validated this turbulent flow model, we can perform further analysis on the atmospheric effects of ultra long pulse LADAR systems.

6. REFERENCES

1. R.G. Lane, et. al., "Simulation of a Kolmogorov phase screen." *Waves in Random Media*, Vol 2, Issue 3, pg 209-224, Imperial College, London. 1992.
2. J. D. Schmidt, *Numerical Simulation of Optical Wave Propagation with Examples in MATLAB*. SPIE Press, 2010.
3. N. Roddier,. "Atmospheric wavefront simulation using Zernike polynomials." Optical Engineering 29(10), Oct. (1990): 1174-1180.
4. R.D. Richmond and S.C. Cain, *Direct Detection LADAR Systems*, SPIE Press, 2010
5. J.W. Goodman, *Statistical Optics*, John Wiley & Sons, Inc., New York, NY, 1985
6. R. J. Noll, "Zernike Polynomials and Atmospheric Turbulence." *Optical Society of America* 66. Mar (1976): 207-11.